OL Organic Letters

pubs.acs.org/OrgLett

Letter

Orthogonal Synthesis of Cationic Azatriphenylene Derivatives for Aggregation-Induced Emission (AIE) and Aggregation-Caused Quenching (ACQ) Property Switching

Published as part of Organic Letters special issue "π-Conjugated Molecules and Materials".

Yushi Ohno,[#] Tsukasa Ehara,[#] Kosuke Sato, Ryoyu Hifumi, Ikuyoshi Tomita, and Shinsuke Inagi*

Cite This: *Org. Lett.* 2025, 27, 4964−4968

Read Online

ACCESS | Metrics & More | Article Recommendations | Supporting Information

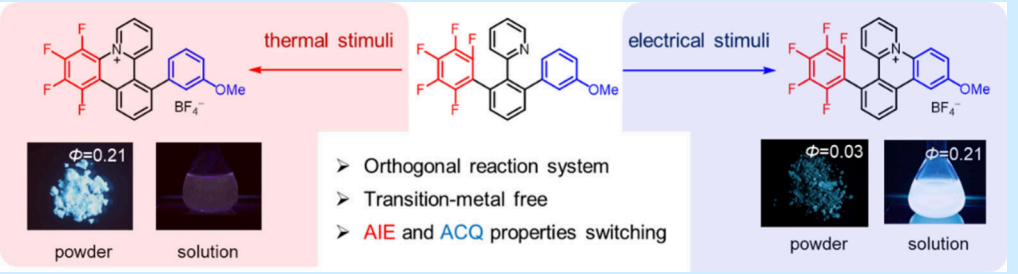

ABSTRACT: Herein, we report a divergent synthesis of cationic azatriphenylene derivatives using orthogonal control of thermal and electro-oxidative pyridination, which transforms the single precursor into controlled products with perfect selectivity. Simultaneously, two switchable reactions afford the corresponding pyridinium salts with different optical properties such as aggregation-induced emission (AIE) and aggregation-caused quenching (ACQ) effects.

Polycyclic aromatic hydrocarbons (PAHs) are two-dimensional (2D) molecules with multiple fused benzene rings and have a broad range of applications in organic and optoelectronic materials based on their diverse structures.[1,2] Heteroatom-doped PAHs, which incorporate heteroatoms into the PAH framework, exhibit unique physical properties depending on the characteristics of the introduced heteroatom.[3] Among them, cationic nitrogen-doped PAHs (N^+-doped PAHs) have been focused in terms of freedom of molecular design by dual strategies with anion/cation species[4−8] and recently applied as organic ionic materials for catalyst,[9−11] light-emitting diode,[12] and bioimaging.[13−16] In this context, the precise synthesis of N^+-doped PAHs has been more important to appropriately design molecular structures and functionalities. One of the most common approaches to N^+-doped PAHs is cyclization reactions with transition-metal-catalyzed C−H activation as the key step,[17−20] which is a powerful yet atom-economical method. However, it is difficult to construct multiple π-conjugated structures from a specific precursor to diversify their physical properties. Therefore, it is required to develop divergent synthetic protocols to lead to versatile products with physical properties from specific precursors.

In divergent synthetic protocols, it is important to selectively obtain only the desired products. Orthogonal transformations are known as a useful approach in selective synthesis and sophisticated reactions that can activate only the desired reaction process without interrupting other reaction systems.[21,22] Recent progress in the use of nonthermal external stimuli such as photo,[23−25] mechanical,[26] and electrical[27] energies for molecular transformations allows for appropriate selection of orthogonal reaction systems, realizing that versatile and complicated π-conjugated structures are accessible from a specific precursor. However, orthogonal transformations for the construction of N^+-doped PAHs are hardly developed because cyclization reactions to produce aromatic rings often require harsh conditions.[28]

In our previous study, we successfully developed two types of intramolecular pyridination protocols to construct cationic azatriphenylene derivatives without the use of a transition-metal catalyst (Figure 1a).[29,30] One is based on the nucleophilic aromatic substitution (S_NAr) reactions driven by thermal stimuli, and the other is based on the anodic pyridination driven by electrical stimuli.[31] In these intramolecular pyridination protocols, there is a high affinity between the electronic properties of the reaction site and the

Received: March 29, 2025
Revised: April 20, 2025
Accepted: April 30, 2025
Published: May 5, 2025

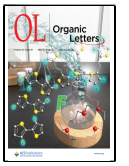

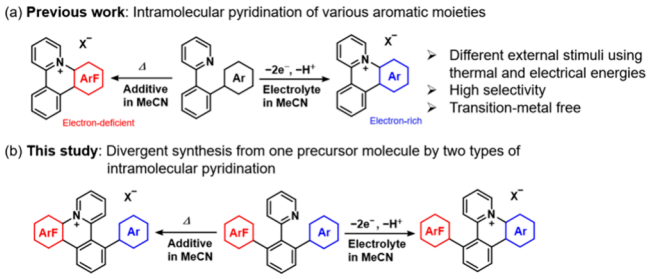

Figure 1. Concept of this study. (a) Intramolecular pyridination of various aromatic moieties. (b) Divergent synthesis from one precursor molecule by two types of intramolecular pyridination.

external stimuli used, e.g., thermal and electrical stimuli activate electron-deficient and electron-rich aromatic moieties, respectively, for cyclization. In this study, we designed a molecular platform for the divergent synthesis of cationic azatriphenylene derivatives via orthogonal control of the thermal and electro-oxidative pyridination (Figure 1b). In addition, we found interesting differences in the optical properties of the obtained products.

Phenylpyridine precursor **1** was subjected to orthogonal transformations (Figure 2). For the thermal S_NAr reaction,

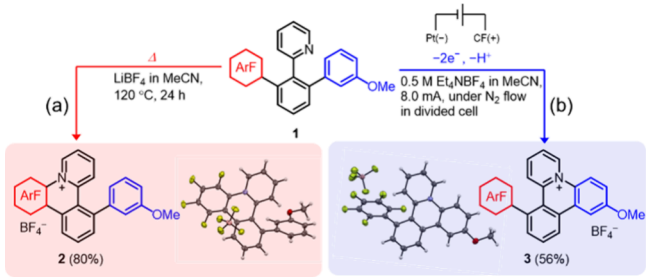

Figure 2. (a) Thermal pyridination of **1**, including the crystal structure of products **2**. (b) Electro-oxidative pyridination of **1**, including the crystal structure of products **3**.

precursor **1** was treated in acetonitrile (MeCN) at 120 °C for 24 h in the presence of lithium tetrafluoroborate ($LiBF_4$). Intramolecular pyridination selectively proceeded on the pentafluorophenyl moiety to afford pyridinium salt **2** containing BF_4^- as the counteranion in 80% isolated yield, where the eliminating fluoride ion was captured by the lithium ion (Figure 2a). For the electrochemical pyridination, we first measured cyclic voltammetry of precursor **1**. The voltammogram showed an irreversible oxidation peak (E_{onset}^{ox} = 1.5 V vs saturated calomel electrode (SCE)), suggesting that the methoxyphenyl moiety is easily oxidized to generate its radical cation and subsequently reacts with the pyridine moiety (Figure S1a). Accordingly, the anodic pyridination of precursor **1** was carried out in the MeCN solution containing 0.5 M tetraethylammonium tetrafluoroborate (Et_4NBF_4) in a H-type divided cell equipped with a carbon felt anode, and a Pt plate cathode. Constant-current electrolysis at 8.0 mA for 2.8 F mol^{-1} afforded product **3** in 63% NMR yield (56% isolated yield) (Figure 2b). In addition, the regioselectivity of the pyridination on the methoxyphenyl moiety can be explained based on DFT calculations. The position where the pyridination took place was consistent with the carbon atom having a large β-LUMO coefficient and natural bond orbital (NBO) spin density in the radical cation state of **1** (Figure S1b). Indeed, any side products, including regioisomers, were not observed in the ^{1}H NMR spectrum of the crude material (Figure S2). The structures of products **2** and **3** were characterized by NMR, high-resolution mass spectrometry (HRMS), and XRD analysis. Furthermore, the thermal pyridination product **2** was not detected at all in the electro-oxidative conditions (and vice versa). These results indicate that the two types of pyridination protocols are orthogonally switchable for a multiresponsive molecule **1** by using thermal or electrical stimuli.

Next, the electrochemical and optical properties of compounds **1**−**3** were investigated, and all data are summarized in Figure 3 and Table 1. The cyclic voltammo-

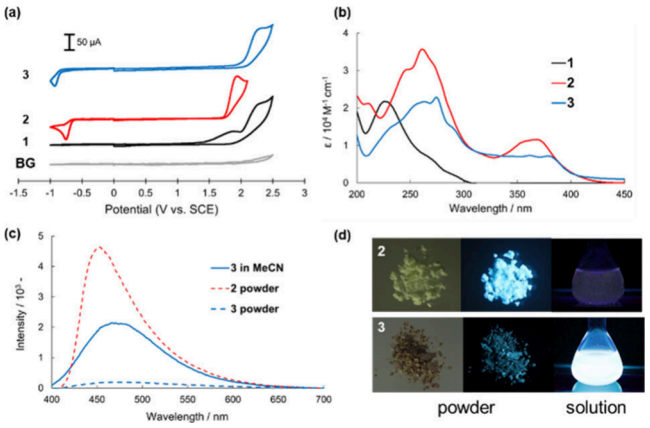

Figure 3. (a) Cyclic voltammograms of **1**−**3** (3 mM) in 0.1 M Bu_4NPF_6/MeCN using a Pt working electrode (φ = 3 mm) at a scan rate of 100 mV/s. The graphs are plotted according to the IUPAC convention. (b) UV−vis absorption for **1**−**3** in MeCN solutions. (c) Fluorescence spectra for **2** in the solid state and **3** in MeCN solution and the solid state. (d) Photographs of **2** and **3** under ambient light (left) and UV irradiation (middle, right).

grams of **2** and **3** showed an irreversible reduction peak in the negative potential region (Figure 3a). This result is due to the electron-deficient nature of the pyridinium moiety and indicates that the reduced species of **2** and **3** are unstable to undergo side reactions such as dimerization.[32] On the other hand, the oxidation peaks observed in the voltammograms of **2** and **3** are shifted to a positive region due to the strong electron-withdrawing nature of the cationic azatriphenylene moiety. More specifically, the reduction potential of **3** was observed in a more negative region compared to that of **2** because the resonance effect of the methoxyphenyl moiety affected the pyridinium moiety in **3**. By contrast, the oxidation potential of **3** was shifted to a more positive region compared to that of **2** because the oxidation of the methoxyphenyl moiety was strongly influenced by the inductive effect of the pyridinium moiety. Therefore, the HOMO−LUMO energy gap of **2** was smaller than that of **3**, as supported by DFT calculations (Figure S3).

The UV−vis absorption maxima of **2** and **3** around 200−300 nm were red-shifted compared to that of precursor **1** due to the π-extension in the fused ring structures; in addition, weak absorption bands appeared in the longer wavelength region in the spectra of **2** and **3** (Figure 3b). The former absorption is attributed to the π−π^* transition, and the latter is the intramolecular charge transfer (ICT) transition from the electron-donating moiety (i.e., methoxyphenyl unit) to the

https://doi.org/10.1021/acs.orglett.5c01277
Org. Lett. 2025, 27, 4964−4968

Table 1. Summary of the Optical and Electrochemical Properties of Compounds 1−3

	λ_{max}^{abs} (nm)[a]		λ_{max}^{em} (nm)[b]		Φ_{FL}[c]				
Compd	$\pi-\pi^*$	ICT	solution	powder	solution	powder	E_{onset}^{red} (V vs SCE)[d]	E_{onset}^{ox} (V vs SCE)[d]	$\Delta E_{HOMO-LUMO}$ (eV)[e]
1	226	–	n.d.[f]	n.d.[f]	n.d.[f]	n.d.[f]	n.d.[f]	1.49	–
2	261	368	n.d.[f]	452	n.d.[f]	0.21	−0.66	1.76	2.42
3	274	363	467	469	0.21	0.03	−0.83	1.98	2.81

[a] λ_{max}^{abs} indicates the absorption maximum wavelength for $\pi-\pi^*$ and intramolecular charge transfer (ICT) absorption measured in solution. [b] λ_{max}^{em} indicates the wavelength of an emission peak in a fluorescence spectrum. [c] Φ_{FL} indicates the internal quantum efficiency in solution using the integrating sphere method. [d] Reduction and oxidation onset potentials determined by CV measurement. [e] HOMO−LUMO gap was estimated by the equations: $\Delta E_{HOMO-LUMO} = E^{ox} - E^{red}$. [f] Not detected.

electron-accepting moiety (i.e., pyridinium unit), as supported by the time-dependent DFT (TD-DFT) calculations (Figures S5 and S6).

Interestingly, there were remarkable differences between the emission behavior of **2** and **3** (Figure 3c). In the fluorescence (FL) measurement in MeCN solution, **2** was a nonemissive species (Figure S8), whereas **3** showed a broad nonstructured emission (λ_{em} = 460 nm) characterized by a donor−acceptor (D−A) type molecule. The quantum efficiency of **3** (Φ_{FL} = 0.21) in MeCN was lower than that of the cationic azatriphenylene derivative bearing the methoxy group (Φ_{FL} = 0.57) in our previous report[30] The lower FL intensity of **3** was probably due to undergoing the nonradiative relaxation induced by the free rotation of the pentafluorophenyl group. The different emission behaviors between **2** and **3** in MeCN were supported by TD-DFT calculations; the oscillatory force (f = 0.0597) of the $S_1 \rightarrow S_0$ transition in **2** was significantly lower than that of **3** (f = 0.3425) (Figure S7). The ICT transition from the pyridinium unit to the methoxyphenyl unit contributed significantly to the $S_1 \rightarrow S_0$ transition in both compounds. Therefore, the fluorescence quenching of **2** was caused by the small orbital overlap between the pyridinium unit and the methoxyphenyl unit. By contrast, the quantum efficiency of powder **2** was Φ_{FL} = 0.21, whereas the fluorescence of powder **3** was Φ_{FL} = 0.03. Compound **2** exhibited emission behavior (λ_{max}^{em} = 531 nm, Φ_{FL} = 0.06) even in the amorphous state by sufficient grinding of pristine **2** (Figure S9), while ground sample **3** was completely quenched (Figure S10). This interesting result suggests that opposite optical properties, i.e., the aggregation-induced emission (AIE) properties for **2** and the aggregation-caused quenching (ACQ) properties for **3** (Figure 3d).

Next, single-crystal X-ray diffraction analysis was performed to investigate the difference in the emission behavior between pyridinium salts **2** and **3** in the solid state (Figure 4). The crystal structure of **2** has a distorted triphenylene unit due to the large torsion angle (27.9°) between the pyridinium moiety and the perfluorophenyl moiety. On the other hand, the crystal structure of **3** has a relatively highly planar triphenylene unit due to the small torsion angles (8.7° and 11.1°) between the pyridinium moiety and the methoxyphenyl moiety (Figure 4a,b). Therefore, it was suggested that **3** is well stacked by π-π interactions with neighboring cation species compared to **2** with the twisted geometry.

To further understand the crystal structures of **2** and **3** in detail, Hirshfeld surface analysis[33,34] was performed. According to the mapped curvedness properties of **2** and **3**, the azatriphenylene unit of **3** has a relatively flat surface compared to that of **2** (Figure 4c,d). Furthermore, the shape-index surfaces of **3** exhibited the pattern of blue and red triangles attributed to the offset $\pi-\pi$ stacking interactions between the

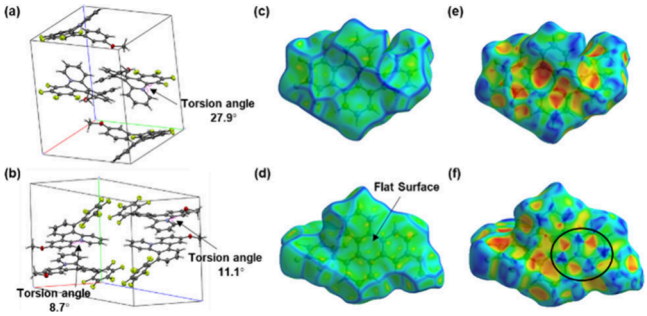

Figure 4. Crystal structures of (a) **2** and (b) **3** (excluding counteranion and solvent). Hirshfeld surfaces mapped with curvedness surfaces of (c) **2** and (d) **3** in the color range from −4.0 au (green, flatness) to 0.4 au (blue, curvedness), and shape-index surfaces of (e) **2** and (f) **3** in the color range from −1.0 au (red, concave) to 1.0 au (blue, convex). The black ellipse represents the repeating pattern of blue and red triangles on the shape-index surface.

neighboring azatriphenylene units, whereas **2** did not exhibit these triangle patterns (Figure 4e,f). Therefore, it was revealed that $\pi-\pi$ interactions are involved effectively in the crystal of **3**. On the other hand, in the 2D fingerprint plot surfaces of **2**, the characteristic spike (d_e = 1.296 Å; d_i = 1.581 Å) attributed to the C (π^+)···F (BF_4^-) interaction was observed, indicating the presence of anion−π^+ interactions in the crystal of **2** (Figure S11).

Based on these considerations, the fluorescence quenching of **3** in the aggregated state should be caused by the energy transfer in the π-stacked structure. In contrast, the fluorescence of **2** in the aggregated state is observed due to the suppression of intermolecular $\pi-\pi$ stacking by the presence of strong anion−π^+ interactions.[35−37] Therefore, the use of anion−π^+ interactions instead of $\pi-\pi$ interactions would be an informative strategy to induce AIE properties in π-conjugated systems. Even though products **2** and **3** consist of the common structure, i.e., aryl-substituted cationic azatriphenylene, the difference in the intermolecular interactions resulted in the different crystal packing with characteristic optical properties. The proposed orthogonal synthetic method with different external stimuli could be a useful way to switch the AIE and ACQ products from precursor **1**.

In conclusion, we have demonstrated the divergent synthesis of cationic azatriphenylene derivatives via orthogonal control of the thermal and electro-oxidative pyridination. The two switchable intramolecular pyridination protocols can transform the single precursor into the corresponding products with complete selectivity. The pyridinium salt products were found to have different optical properties such as AIE and ACQ effects. In addition, we successfully elucidated the origin of the different fluorescence behavior in solution and the solid state

https://doi.org/10.1021/acs.orglett.5c01277
Org. Lett. 2025, 27, 4964−4968

by theoretical calculation and Hirshfeld surface analysis. This orthogonal control method is expected to be developed not only as a divergent synthetic strategy but also as a methodology for designing novel stimuli-responsive AIEgens.[38]

■ ASSOCIATED CONTENT

Data Availability Statement

The data underlying this study are available article and its Supporting Information.

Supporting Information

The Supporting Information is available free of charge at https://pubs.acs.org/doi/10.1021/acs.orglett.5c01277.

Detailed experimental procedures, characterization data, DFT studies, single-crystal X-ray data, and copies of NMR spectra (PDF)

Accession Codes

Deposition Numbers 2347850−2347851 contain the supplementary crystallographic data for this paper. These data can be obtained free of charge via the joint Cambridge Crystallographic Data Centre (CCDC) and Fachinformationszentrum Karlsruhe Access Structures service.

■ AUTHOR INFORMATION

Corresponding Author

Shinsuke Inagi − *Department of Chemical Science and Engineering, School of Materials and Chemical Technology, Institute of Science Tokyo, Yokohama, Kanagawa 226-8501, Japan;* orcid.org/0000-0002-9867-1210; Email: inagi@mct.isct.ac.jp

Authors

Yushi Ohno − *Department of Chemical Science and Engineering, School of Materials and Chemical Technology, Institute of Science Tokyo, Yokohama, Kanagawa 226-8501, Japan*

Tsukasa Ehara − *Department of Chemical Science and Engineering, School of Materials and Chemical Technology, Institute of Science Tokyo, Yokohama, Kanagawa 226-8501, Japan*

Kosuke Sato − *Department of Chemical Science and Engineering, School of Materials and Chemical Technology, Institute of Science Tokyo, Yokohama, Kanagawa 226-8501, Japan;* orcid.org/0000-0003-3914-0249

Ryoyu Hifumi − *Department of Chemical Science and Engineering, School of Materials and Chemical Technology, Institute of Science Tokyo, Yokohama, Kanagawa 226-8501, Japan;* orcid.org/0000-0002-3913-1214

Ikuyoshi Tomita − *Department of Chemical Science and Engineering, School of Materials and Chemical Technology, Institute of Science Tokyo, Yokohama, Kanagawa 226-8501, Japan*

Complete contact information is available at: https://pubs.acs.org/10.1021/acs.orglett.5c01277

Author Contributions

#Y.O. and T.E. contributed equally.

Notes

The authors declare no competing financial interest.

■ ACKNOWLEDGMENTS

This research was supported by a Grant-in-Aid for Transformative Research Areas (A) Green Catalysis Science for Renovating Transformation of Carbon-Based Resources (Green Catalysis Science) (MEXT KAKENHI Grants JP23H-04914) from MEXT. We are thankful for the support of a Tokyo Tech Advanced Researchers (STAR) grant funded by the Tokyo Institute of Technology Fund (Tokyo Tech Fund, for S.I.), and a JST SPRING grant (No. JPMJSP2106, for Y.O.) from JST. Y.O. acknowledges support from the Kato Foundation for Promotion of Science (KS-3501). We thank Dr. Yoshihisa Sei (single-crystal X-ray analysis) and Dr. Masato Koizumi (HR-MS) at Materials Analysis Division, Core Facility Center, Institute of Science Tokyo.

■ REFERENCES

(1) Wu, J.; Pisula, W.; Müllen, K. Graphenes as Potential Material for Electronics. *Chem. Rev.* **2007**, *107*, 718−747.

(2) Narita, A.; Wang, X. Y.; Feng, X.; Müllen, K. New Advances in Nanographene Chemistry. *Chem. Soc. Rev.* **2015**, *44*, 6616−6643.

(3) Borissov, A.; Maurya, Y. K.; Moshniaha, L.; Wong, W. S.; Żyła-Karwowska, M.; Stępień, M. Recent Advances in Heterocyclic Nanographenes and Other Polycyclic Heteroaromatic Compounds. *Chem. Rev.* **2022**, *122*, 565−788.

(4) Wu, D.; Zhi, L.; Bodwell, G. J.; Cui, G.; Tsao, N.; Müllen, K. Self-Assembly of Positively Charged Discotic PAHs: From Nanofibers to Nanotubes. *Angew. Chem., Int. Ed.* **2007**, *46*, 5417−5420.

(5) Wu, D.; Feng, X.; Takase, M.; Haberecht, M. C.; Müllen, K. Synthesis and Self-Assembly of Dibenzo[Jk,Mn]Naphtho[2,1,8-Fgh]-Thebenidinium Derivates. *Tetrahedron* **2008**, *64*, 11379−11386.

(6) Wu, D.; Pisula, W.; Enkelmann, V.; Feng, X.; Müllen, K. Controllable Columnar Organization of Positively Charged Polycyclic Aromatic Hydrocarbons by Choice of Counterions. *J. Am. Chem. Soc.* **2009**, *131*, 9620−9621.

(7) Wu, D.; Liu, R.; Pisula, W.; Feng, X.; Müllen, K. Two-Dimensional Nanostructures from Positively Charged Polycyclic Aromatic Hydrocarbons. *Angew. Chem., Int. Ed.* **2011**, *50*, 2791−2794.

(8) Yang, C.; Wu, D.; Zhao, W.; Ye, W.; Xu, Z.; Zhang, F.; Feng, X. Anion-Induced Self-Assembly of Positively Charged Polycyclic Aromatic Hydrocarbons towards Nanostructures with Controllable Two-Dimensional Morphologies. *CrystEngComm* **2016**, *18*, 877−880.

(9) Fukuzumi, S.; Kotani, H.; Ohkubo, K.; Ogo, S.; Tkachenko, N. V.; Lemmetyinen, H. Electron-Transfer State of 9-Mesityl-10-Methylacridinium Ion with a Much Longer Lifetime and Higher Energy Than That of the Natural Photosynthetic Reaction Center. *J. Am. Chem. Soc.* **2004**, *126*, 1600−1601.

(10) Karak, P.; Mandal, S. K.; Choudhury, J. Bis-Imidazolium-Embedded Heterohelicene: A Regenerable NADP+ Cofactor Analogue for Electrocatalytic CO2 Reduction. *J. Am. Chem. Soc.* **2023**, *145*, 7230−7241.

(11) Karak, P.; Mandal, S. K.; Choudhury, J. Exploiting the NADP +/NADPH-like Hydride-Transfer Redox Cycle with Bis-Imidazolium-Embedded Heterohelicene for Electrocatalytic Hydrogen Evolution Reaction. *J. Am. Chem. Soc.* **2023**, *145*, 17321−17328.

(12) Chen, K.; Li, G.; Zhang, H.; Wu, H.; Li, Y.; Li, Y.; Wang, Z.; Tang, B. Z. Construction of Sublimable Pure Organic Ionic Material with High Solid Luminescence Efficiency Based on Anion-Π+ Interactions Tuning Strategy. *Chem. Eng. J.* **2022**, *433*, 133646−133655.

(13) Ihmels, H. Invited Review Intercalation of Organic Dye Molecules into Double-Stranded DNA. Part 2: The Annelated Quinolizinium Ion as a Structural Motif in DNA Lntercalatorst. *Photochem. Photobiol.* **2005**, *81*, 1107−1115.

(14) Suárez, R. M.; Bosch, P.; Sucunza, D.; Cuadro, A. M.; Domingo, A.; Mendicuti, F.; Vaquero, J. J. Targeting DNA with Small Molecules: A Comparative Study of a Library of Azonia Aromatic Chromophores. *Org. Biomol. Chem.* **2015**, *13*, 527−538.

(15) Bosch, P.; Sucunza, D.; Mendicuti, F.; Domingo, A.; Vaquero, J. J. Dibenzopyridoimidazocinnolinium Cations: A New Family of Light-up Fluorescent DNA Probes. *Organic Chemistry Frontiers* **2018**, *5* (12), 1916−1927.
(16) Li, Q. Q.; Hamamoto, Y.; Kwek, G.; Xing, B.; Li, Y.; Ito, S. Diazapentabenzocorannulenium: A Hydrophilic/Biophilic Cationic Buckybowl. *Angew. Chem., Int. Ed.* **2022**, *61*, No. e202112638.
(17) Nuñez, A.; Abarca, B.; Cuadro, A. M.; Alvarez-Builla, J.; Vaquero, J. J. Ring-Closing Metathesis Approach to Heteroaromatic Cations: Synthesis of Benzo[a]Quinolizinium Salts. *Eur. J. Org. Chem.* **2011**, *2011*, 1280−1290.
(18) Castillo, R. R.; Burgos, C.; Vaquero, J. J.; Alvarez-Builla, J. Radical Intramolecular Arylation of Pyridinium Salts: A Straightforward Entry to 7-Hydroxypyrido[2,1-a]Isoquinolinylium Salts. *Eur. J. Org. Chem.* **2011**, *2011*, 619−628.
(19) Paroi, B.; Sancheti, S. P.; Patil, N. T. 1,2-Aminofunctionalization Reactions of Pyridino-Alkynes via Carbophilic Activation. *Chem. Rec.* **2021**, *21*, 3779−3794.
(20) Hsiao, H. C.; Li, M. C.; Vedarethinam, G.; Chen, P. L.; Chuang, S. C. Synthesis of Benzo[c]Cinnolinium Salts from 2-Azobiaryls by Copper(II) or Electrochemical Oxidation. *Org. Lett.* **2024**, *26*, 1694−1698.
(21) Wong, C.-H.; Zimmerman, S. C. Orthogonality in Organic, Polymer, and Supramolecular Chemistry: From Merrifield to Click Chemistry. *Chem. Commun.* **2013**, *49*, 1679−1695.
(22) Corrigan, N.; Boyer, C. 100th Anniversary of Macromolecular Science Viewpoint: Photochemical Reaction Orthogonality in Modern Macromolecular Science. *ACS Macro Lett.* **2019**, *8*, 812−818.
(23) Jiang, X.; Zeng, Z.; Hua, Y.; Xu, B.; Shen, Y.; Xiong, J.; Qiu, H.; Wu, Y.; Hu, T.; Zhang, Y. Merging C-H Vinylation with Switchable 6π-Electrocyclizations for Divergent Heterocycle Synthesis. *J. Am. Chem. Soc.* **2020**, *142*, 15585−15594.
(24) Jiang, X.; Zeng, Z.; Shi, D.; Liu, C.; Zhang, Y. Divergent Total Syntheses of Pseudoberberine and Nitidine through C[Sbnd]H Vinylation and Switchable 6π Electrocyclizations. *Tetrahedron Lett.* **2021**, *66*, 152839−152842.
(25) Liu, T.; Qi, C.; Zhou, Q.; Dai, W.; Lan, Y.; Xu, L.; Ren, J.; Pan, Y.; Yang, L.; Ge, Y.; Qu, Y. K.; Li, W.; Li, H.; Xiao, S. Divergent Synthesis of Contorted Polycyclic Aromatics Containing Pentagons, Heptagon, and/or Azulene. *Org. Lett.* **2022**, *24*, 472−477.
(26) Luo, H.; Liu, F. Z.; Liu, Y.; Chu, Z.; Yan, K. K. Biasing Divergent Polycyclic Aromatic Hydrocarbon Oxidation Pathway by Solvent-Free Mechanochemistry. *J. Am. Chem. Soc.* **2023**, *145*, 15118−15127.
(27) Lu, P.; Zhuang, W.; Lu, L.; Liu, A.; Chen, Y.; Wu, C.; Zhang, X.; Huang, Q. Chemodivergent Synthesis of Indeno[1,2- b]Indoles and Isoindolo[2,1- a]Indoles via Mn(III)-Mediated or Electrochemical Intramolecular Radical Cross-Dehydrogenative Coupling. *J. Org. Chem.* **2022**, *87*, 10967−10981.
(28) Shaikh, A. C.; Banerjee, S.; Mule, R. D.; Bera, S.; Patil, N. T. External Oxidant-Dependent Reactivity Switch in Copper-Mediated Intramolecular Carboamination of Alkynes: Access to a Different Class of Fluorescent Ionic Nitrogen-Doped Polycyclic Aromatic Hydrocarbons. *J. Org. Chem.* **2019**, *84*, 4120−4130.
(29) Asanuma, Y.; Eguchi, H.; Nishiyama, H.; Tomita, I.; Inagi, S. Synthesis of Ring-Fused Pyridinium Salts by Intramolecular Nucleophilic Aromatic Substitution Reaction and Their Optoelectronic Properties. *Org. Lett.* **2017**, *19*, 1824−1827.
(30) Ohno, Y.; Ando, S.; Furusho, D.; Hifumi, R.; Nagata, Y.; Tomita, I.; Inagi, S. Synthesis of Cationic Azatriphenylene Derivatives by Electrochemical Intramolecular Pyridination and Characterization of Their Optoelectronic Properties. *Org. Lett.* **2023**, *25*, 3951−3955.
(31) Morofuji, T.; Shimizu, A.; Yoshida, J. I. Electrochemical C-H Amination: Synthesis of Aromatic Primary Amines via N -Arylpyridinium Ions. *J. Am. Chem. Soc.* **2013**, *135*, 5000−5003.
(32) Bruggeman, C.; Gregurash, K.; Hickey, D. P. Impact of Sodium Pyruvate on the Electrochemical Reduction of NAD+ Biomimetics. *Faraday Discuss.* **2023**, *247*, 87−100.
(33) McKinnon, J. J.; Jayatilaka, D.; Spackman, M. A. Towards Quantitative Analysis of Intermolecular Interactions with Hirshfeld Surfaces. *Chem. Commun.* **2007**, 3814−3816.
(34) Spackman, M. A.; Jayatilaka, D. Hirshfeld Surface Analysis. *CrystEngComm.* **2009**, *11*, 19−32.
(35) Wang, J.; Gu, X.; Zhang, P.; Huang, X.; Zheng, X.; Chen, M.; Feng, H.; Kwok, R. T. K.; Lam, J. W. Y.; Tang, B. Z. Ionization and Anion-Π+ Interaction: A New Strategy for Structural Design of Aggregation-Induced Emission Luminogens. *J. Am. Chem. Soc.* **2017**, *139*, 16974−16979.
(36) Jiang, G.; Yu, J.; Wang, J.; Tang, B. Z. Ion−π Interactions for Constructing Organic Luminescent Materials. *Aggregate.* **2022**, *3*, No. e285.
(37) Liu, L.; Gong, J.; Jiang, G.; Wang, J. Anion-Π^+ AIEgens for Fluorescence Imaging and Photodynamic Therapy. *Chem.—Eur. J.* **2024**, *30*, No. e202400378.
(38) Zhang, J.; He, B.; H u, Y.; Alam, P.; Zhang, H.; Lam, J. W. Y.; Tang, B. Z. Stimuli-Responsive AIEgens. *Adv. Mater.* **2021**, *33*, No. 202008071.

https://doi.org/10.1021/acs.orglett.5c01277
Org. Lett. 2025, 27, 4964−4968